The XSTAR Atomic Database

Claudio Mendoza
Physics Center, IVIC,
Caracas

ASOS14
Sorbonne Université, Paris
13/07/23

XSTAR computes the physical conditions and emission spectra of a photoionized gas (Kallman+01, Bautista+01)

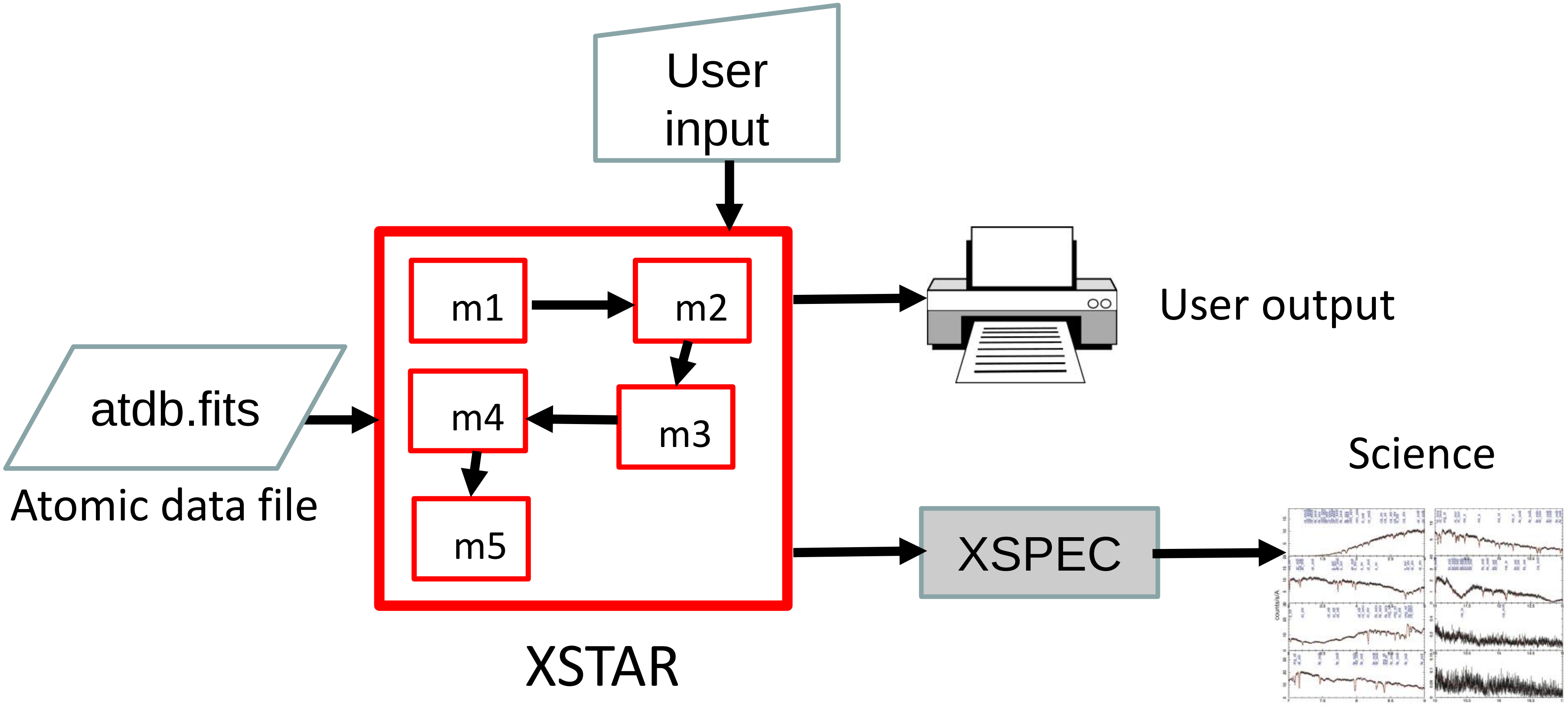

XSTAR atomic database team since 2001 (Mendoza+22)

- Manuel A. Bautista (WMU, NASA, USA)
- Jérôme Deprince (ULB, Belgium)
- Javier A. García (NASA-GSFC, USA)
- Efraín Gatuzz (MPI-EP, Germany)
- Thomas W. Gorczyca (WMU, USA)
- Timothy R. Kallman (NASA-GSFC, USA)
- Claudio Mendoza (IVIC, Venezuela)
- Patrick Palmeri (UMons, Belgium)
- Pascal Quinet (UMons, ULiegè, Belgium)
- Michael C. Witthoeft (NASA-GSFC, ADNET Sys.)

X-ray astronomy comes of age in 1999

Chandra Observatory

Instruments/detectors: High-resolution images with CCDs. Transmission grating spectrometers (0.1 - 10 keV).

Mirror Description: 4 nested pairs with an area of 1145 cm^2 and 0.5 arc sec resolution.

XMM-Newton Observatory

Instruments/detectors: CCD cameras and reflection grating spectrometers (0.1 - 12 keV).

Mirror Description: 3 modules with 58 mini-mirrors each giving a total area of 4300 cm^2 and 5 arc sec resolution.

XRISM will enable the study of X-ray objects with high-resolution spectroscopy and high-throughput imaging

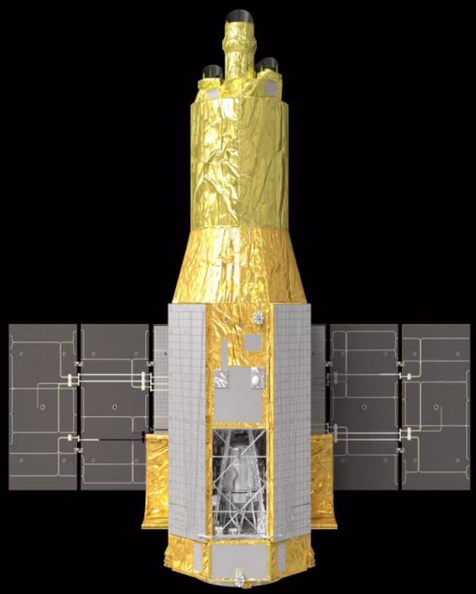

Source: JAXA

Main scientific goals:

- Evolution of the largest structures
- Matter in extreme gravitational fields
- Black-hole spin
- Internal structure of neutron stars
- Particle jets

XRISM soft X-ray spectrometer (SXS) is based on a micro-calorimeter

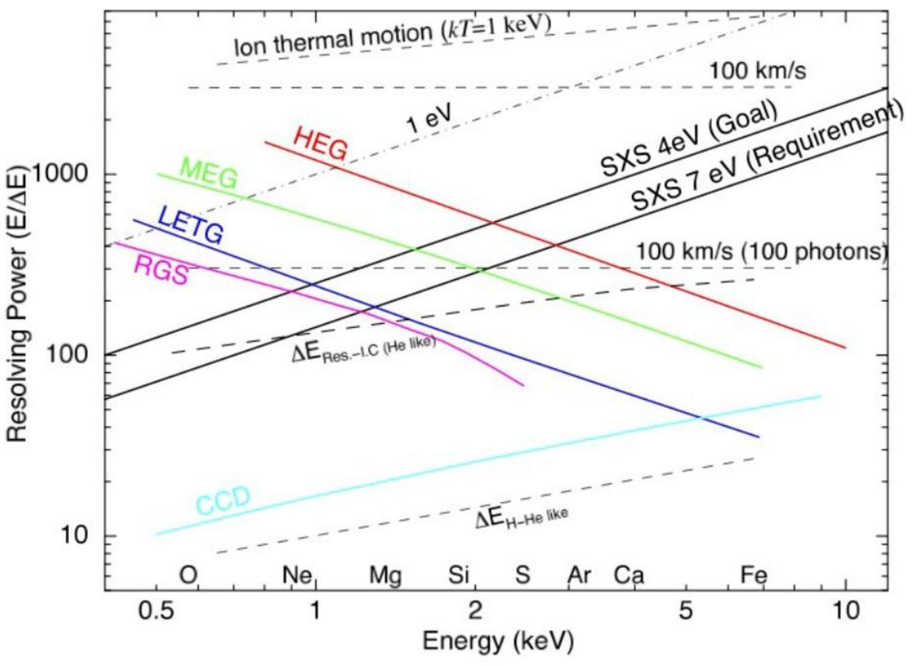

Resolving Power

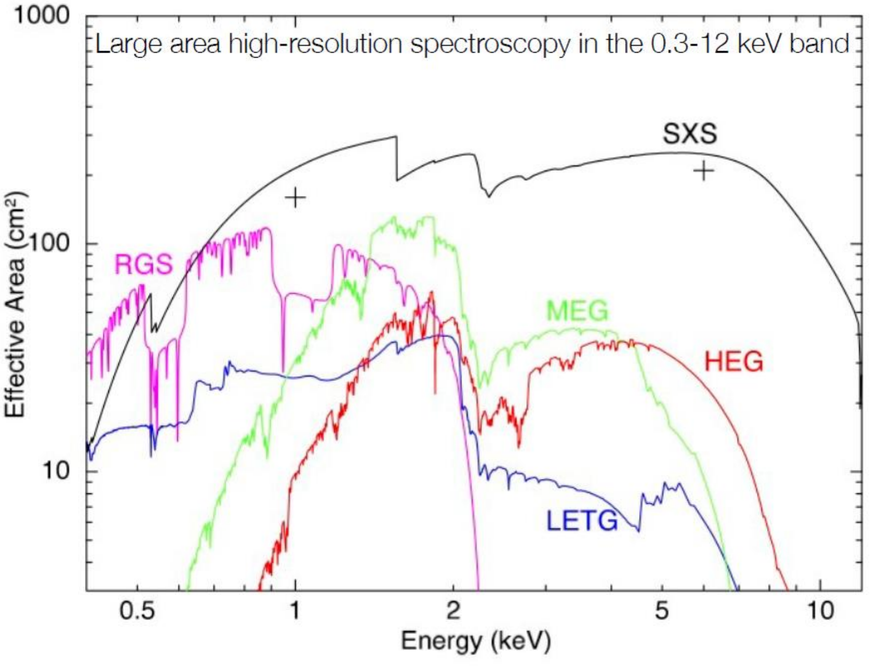

Effective Area

XSTAR database contains targets and data structures to derive rates for ions with $1 \leq Z \leq 30$ and $1 \leq N \leq Z-2$

- Ground state photoionization
- Bound–bound collision
- Bound–bound radiative
- Bound–free collision (level)
- Total recombination
- Bound–free radiative (level)
- Total recombination forcing normalization
- Two-photon decay
- Charge exchange

- Element data
- Ion data
- Level data
- Bound–bound radiative, superlevel to spectroscopic level
- Collisional ionization total rate
- Bound–bound collisional, superlevel to spectroscopic level
- Non-radiative Auger transition
- Inner-shell photoabsorption followed by autoionization.

There are well-known plasma diagnostics based on X-ray line ratios

- H-like: Lyα/Lyβ is a temperature diagnostic
- He-like: $n=2\rightarrow1$ triplet is a temperature and density diagnostic (Gabriel & Jordan 69, Dubau+)

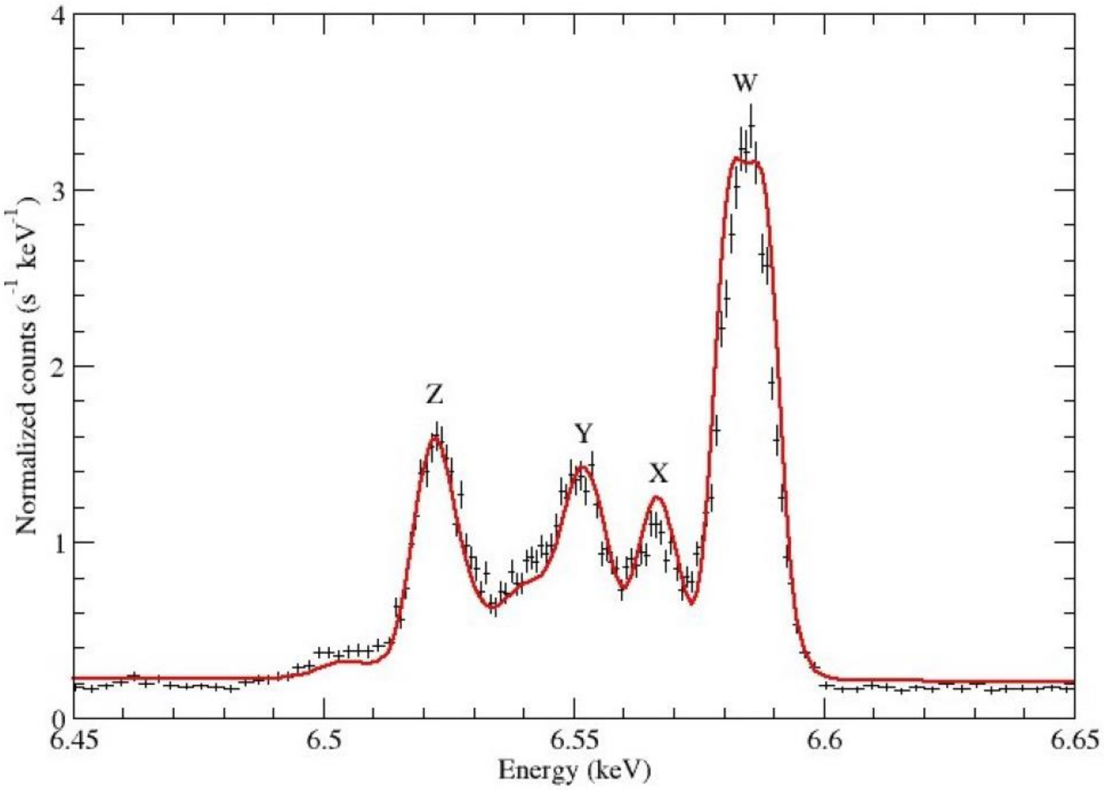

Hitomi spectrum of the Perseus Cluster fitted with XSTAR showing that the He-triplet becomes a quartet (Mendoza+22)

Ne-like: n=3→2 line ratios (15 -17 Å) in Fe XVII are used as density, temperature, and ionization-state diagnostics

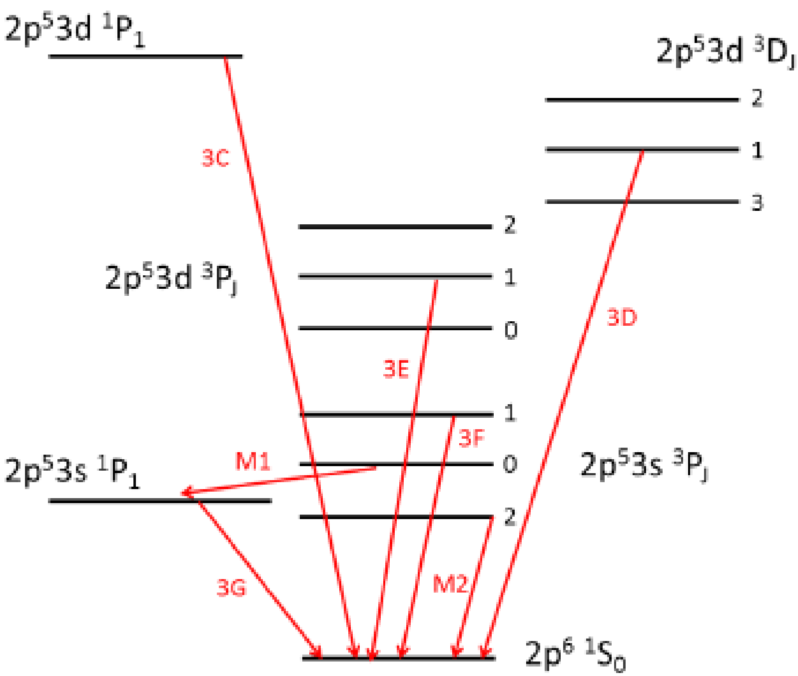

Fe XVII n=2-3 level structure
Figure from Mendoza+17

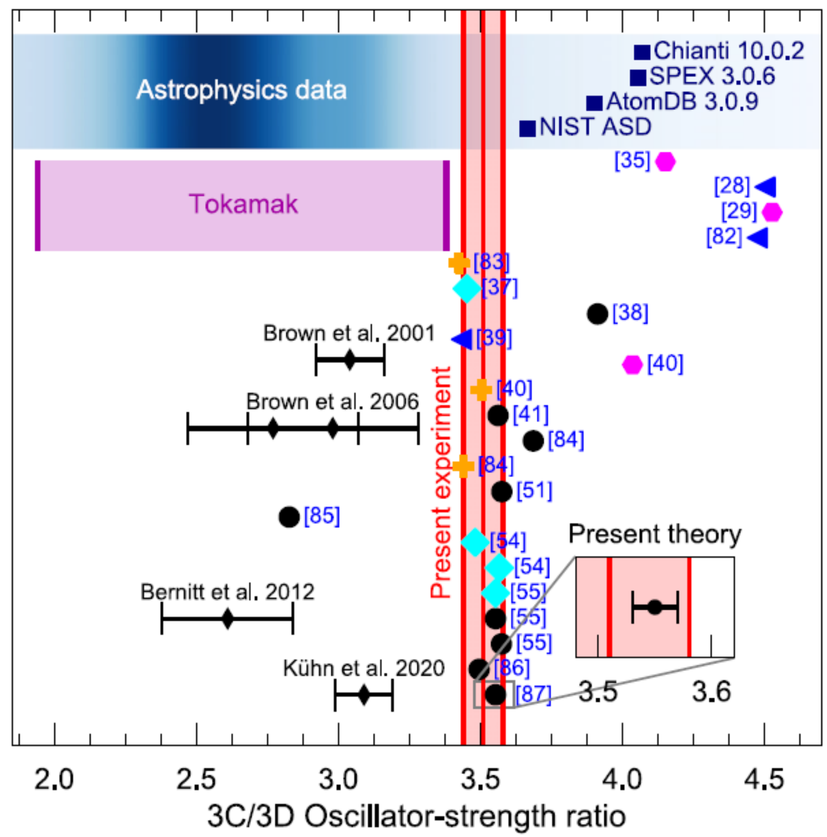

Recent measurement solves the long-standing problem of Fe XVII 3C/3D f-value ratio (Kuhn+22)

A signature interaction of X-rays with ions gives rise to K absorption and emission lines (fluorescence)

Illustrating these processes in the relatively simple case of Ne-like Fe XVII, the photoexcited K-vacancy states

$$h\nu + 1s^2 2s^2 2p^6 \longrightarrow 1s2s^2 2p^6 np \tag{1}$$

have access to the following decay tree:

$$
\begin{aligned}
1s2s^2 2p^6 np \quad & \xrightarrow{Kn} \quad 1s^2 2s^2 2p^6 + h\nu_n && (2)\\
& \xrightarrow{K\alpha} \quad 1s^2 2s^2 2p^5 np + h\nu_\alpha && (3)\\
& \xrightarrow{KLn} \quad \begin{cases} 1s^2 2s^2 2p^5 + e^- \\ 1s^2 2s 2p^6 + e^- \end{cases} && (4)\\
& \xrightarrow{KLL} \quad \begin{cases} 1s^2 2s^2 2p^4 np + e^- \\ 1s^2 2s 2p^5 np + e^- \\ 1s^2 2p^6 np + e^- \end{cases} && (5)
\end{aligned}
$$

A signature interaction of X-rays with ions gives rise to K absorption and emission lines (fluorescence)

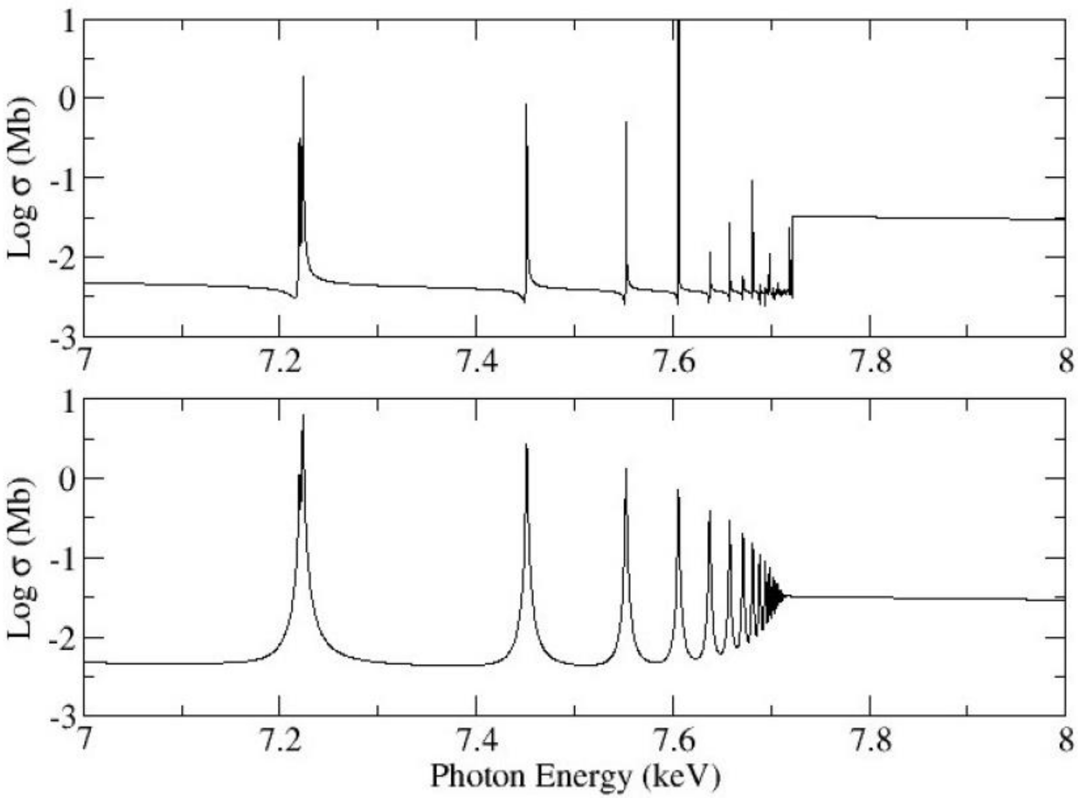

K photoabsorption cross section of Ne-like Fe XVII

Radiation and Auger damping has been included in the *R*-matrix package through an optical potential following formalisms by Hickman-Robicheaux and Davies and Seaton (Gorczyca+99)

Accuracy of photoabsorption cross sections is vital in determining astrophysical inferences

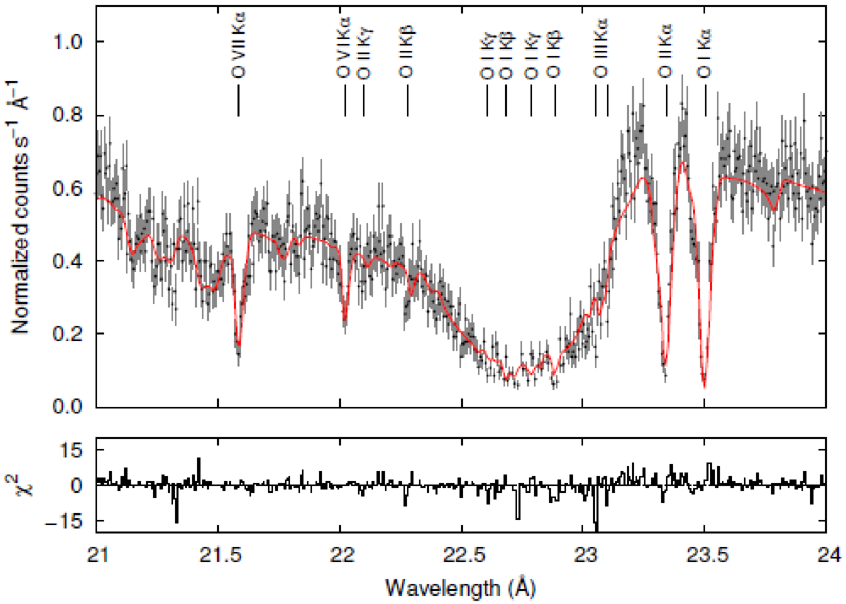

Chandra MEG spectrum of XTE J1817-330

The observed flux can be approximated as

$$F(E) = F_0 \exp\left[-N_{\mathrm{O\,I}}\sigma_{\mathrm{O\,I}}(E)\right]$$

where F_0 is a normalization factor, $N_{\mathrm{O\,I}}$ is the oxygen column density, and $\sigma_{\mathrm{O\,I}}(E)$ is the photoabsorption cross section for neutral oxygen.

Figure from Gatuzz+13

The accuracy of photoabsorption cross sections is vital in determining astrophysical inferences: e.g. O I K lines

Method	Source	E(1s - 2p, eV)	E(1s -3p, eV)	ΔE(eV)
Astronomical observations	*XMM-Newton*, MrK 421 (Gorczyca+13)	527.30(5)	541.95(28)	14.65(33)
	Chandra, 7 sources (Gorczyca+13)	527.44(9)	541.72(18)	14.28(21)
	Chandra, shifted (Gorczyca+13)	527.26(9)		
	Chandra, 11 sources (Liao+13)	527.39(2)		
	Chandra, 6 sources (Juett+04)	527.41(18)	541.77(40)	14.36(58)
Laboratory measurements	HZB (Leutenegger+20)	527.26(4)	541.645(12)	14.39(5)
	ALS (McLaughlin+13)	526.79(4)	541.19(4)	14.40(8)
	ALS (Stolte+97)	526.79(4)	541.20(4)	14.41(8)
	WSRC (Menzel+96)	527.85(10)	541.27(15)	13.41(25)
	Auger spectroscopy (Caldwell+94)	527.20(30)		
Calculation	MCHF (Gorczyca+13)	527.49		

Smearing of the Fe K edge by damping is distinctive in the opacities of a photoionized gas at ξ =10

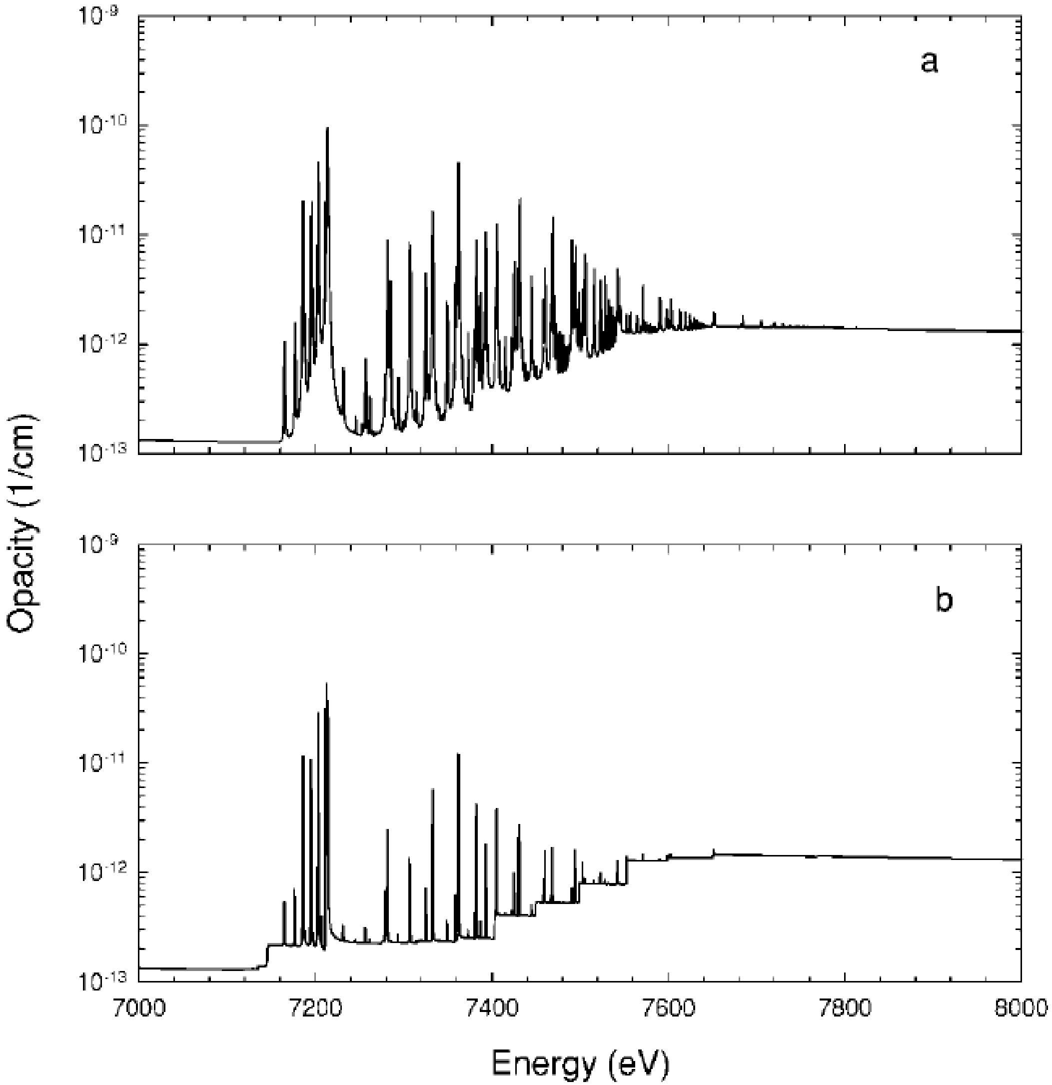

Damping included

No damping

Figure from Palmeri+02

Comparison of I(Kβ/Kα) for Fe ions with 17 ≤ N ≤ 23 can lead to charge-state diagnostics

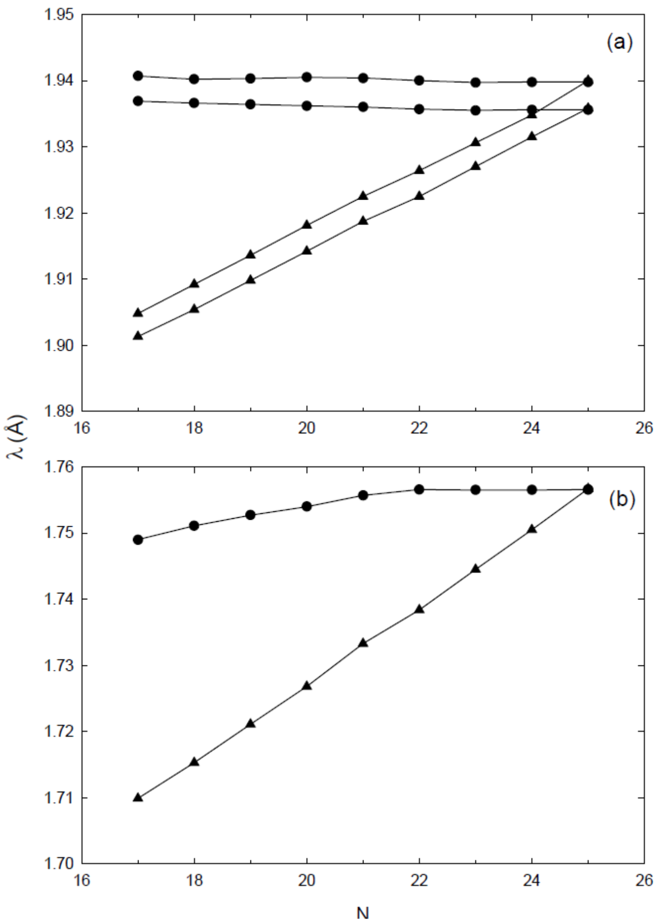

Fig. 1. Comparison of centroid wavelengths for **a)** Kα and **b)** Kβ UTAs in Fe ions with $17 \le N \le 25$. Filled circles: this work. Filled triangles: Kaastra & Mewe (1993).

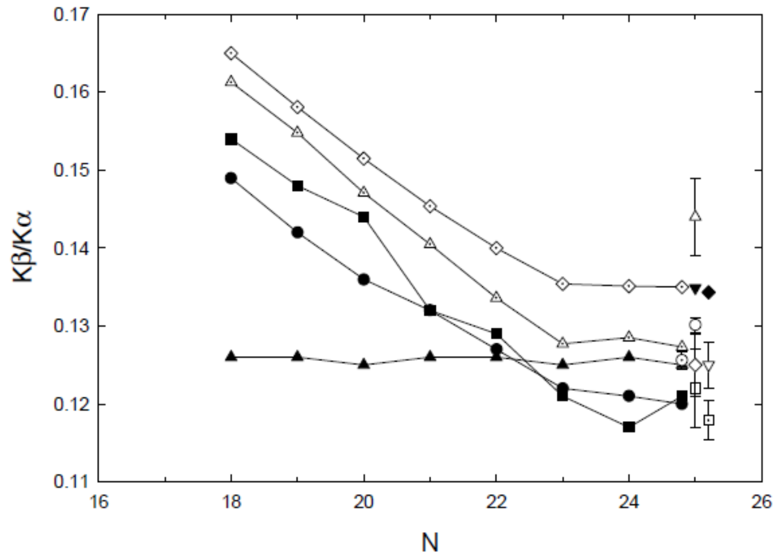

Fig. 2. Comparison of Kβ/Kα intensity ratios for Fe ions with $18 \le N \le 25$. Filled circles: HFR, this work. Dotted upright triangles: AUTOSTRUCTURE, this work. Dotted diamonds: MCDF-SAL, this work. Filled upright triangles: Kaastra & Mewe (1993). Filled squares: Jacobs & Rozsnyai (1986). Filled diamonds: Scofield (1974). Filled inverted triangles: Jankowski & Polasik (1989). Circles: Perujo et al. (1987). Upright triangles: Hölzer et al. (1997). Squares: Rao et al. (1986). Diamonds: Berényi et al. (1978). Inverted triangles: Salem et al. (1972). Dotted circles: Slivinsky & Ebert (1972). Dotted squares: Hansen et al. (1970).

Figures from Palmeri+02

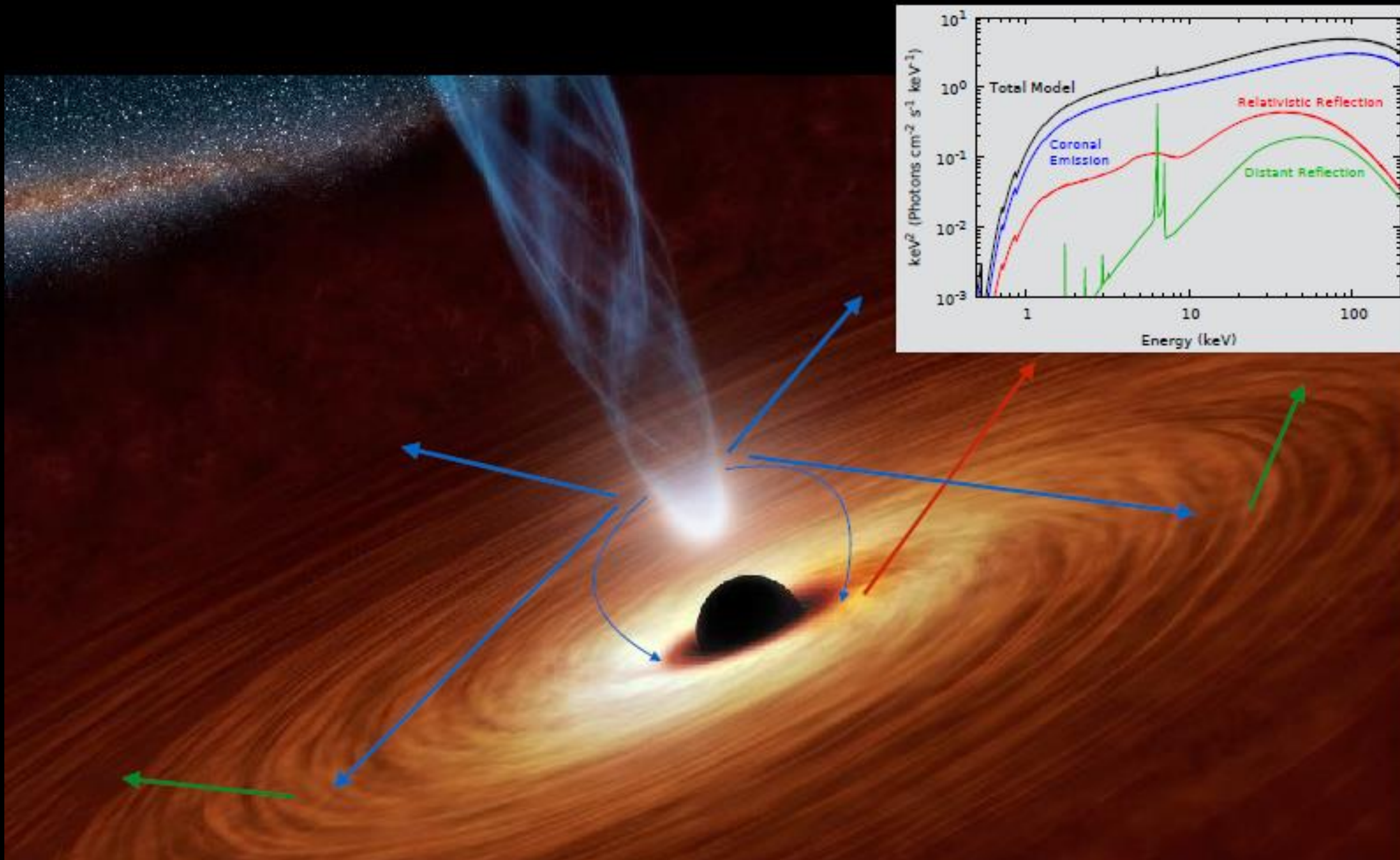

X-ray Reflection from Accretion Disks

RELXILL: Relativistic X-ray Reflection

RELXILL: Relativistic reflection model that combines detailed reflection spectra from **xillver** (García & Kallman 2010), with the **relline** relativistic blurring code (Dauser et al. 2010).

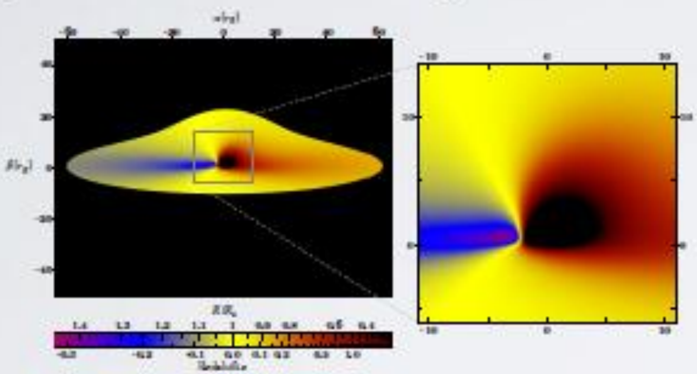

Model Parameters

a: Black hole spin, R_{in}: Disk's inner edge
i: Inclination, ϵ: Emissivity index
R_f: Reflection fraction, Γ: Power-law index
E_{cut}: High-energy cutoff, A_{Fe}: Fe abundance

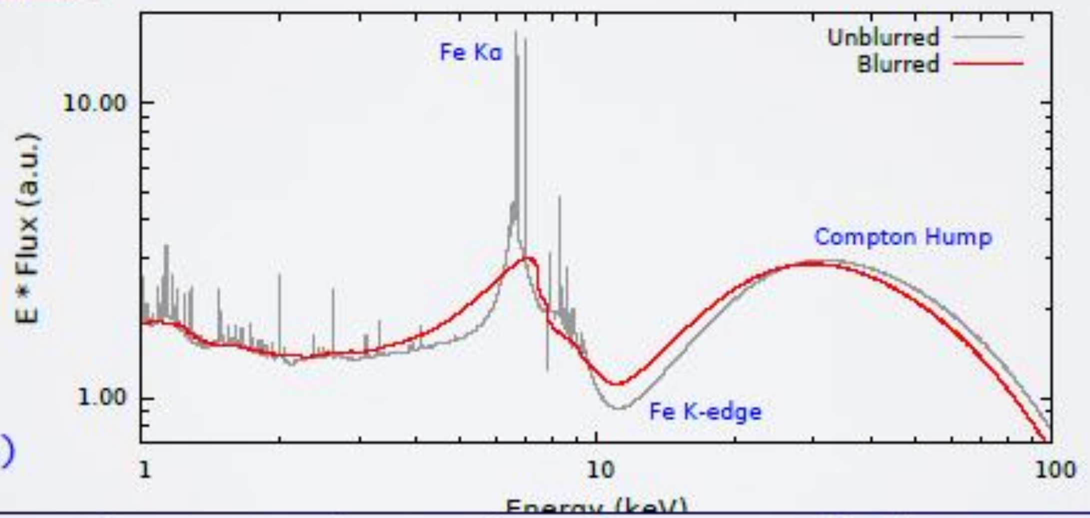

(García+14b)

http://www.sternwarte.uni-erlangen.de/research/relxill/

X-ray Reflection from the Inner-Disk

The line profile of iron K-alpha from MCG-6-30-15 observed by the ASCA satellite (Tanaka et al. 1995)

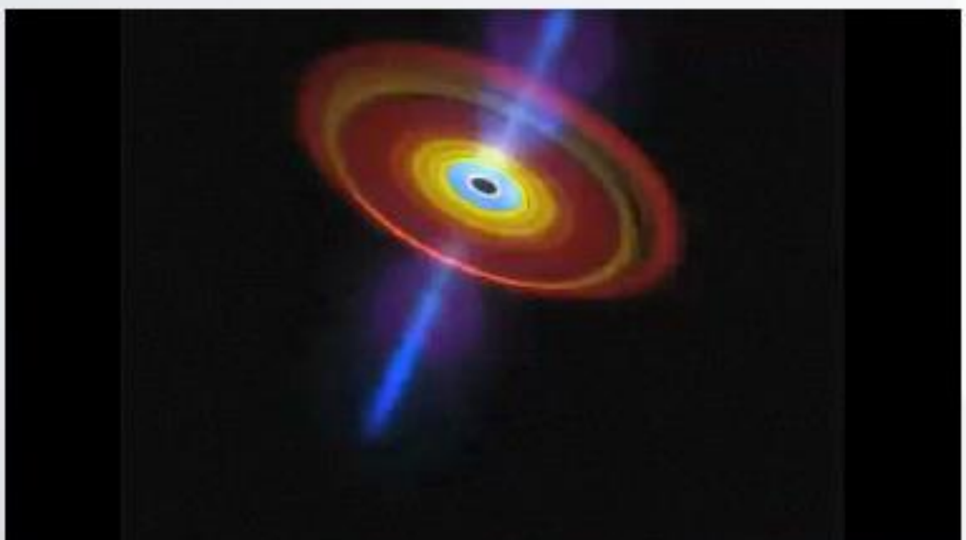

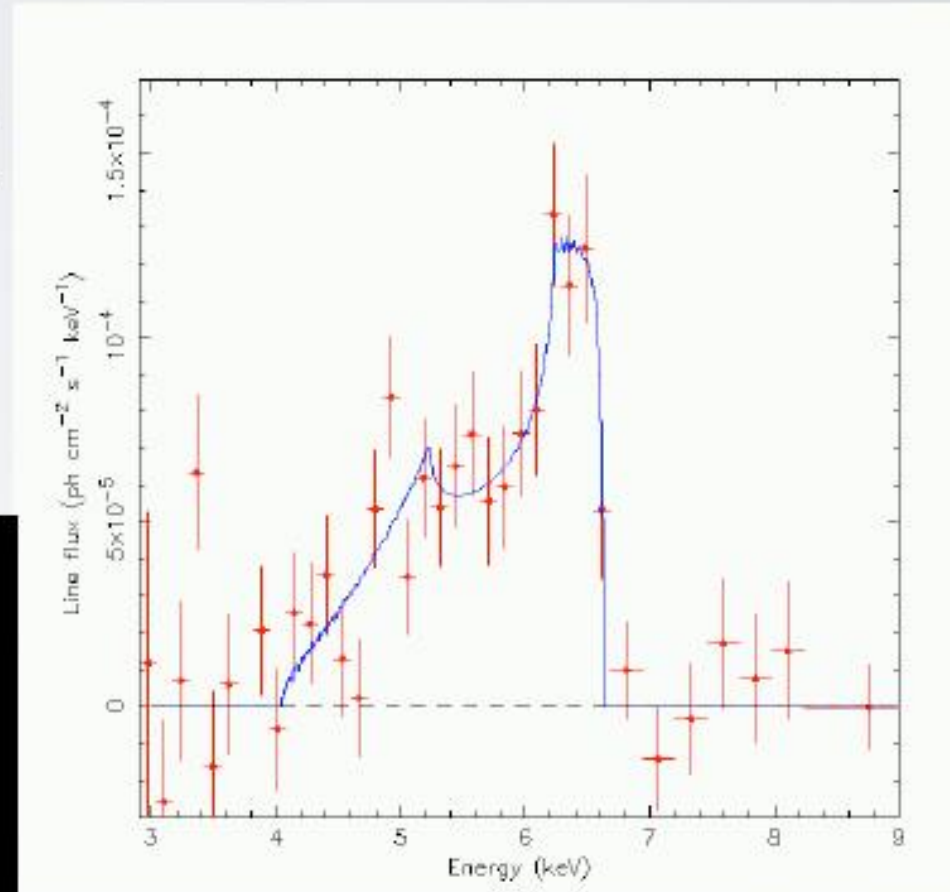

Iron line Profiles near a Black Hole

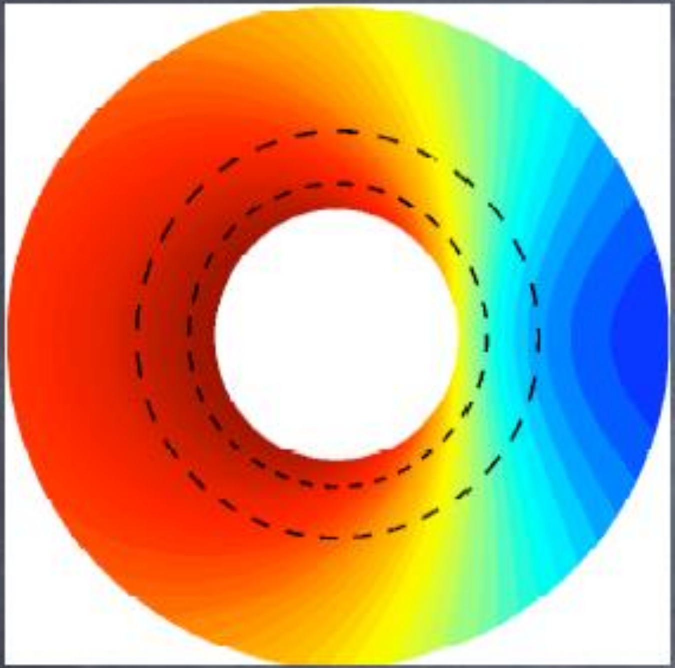

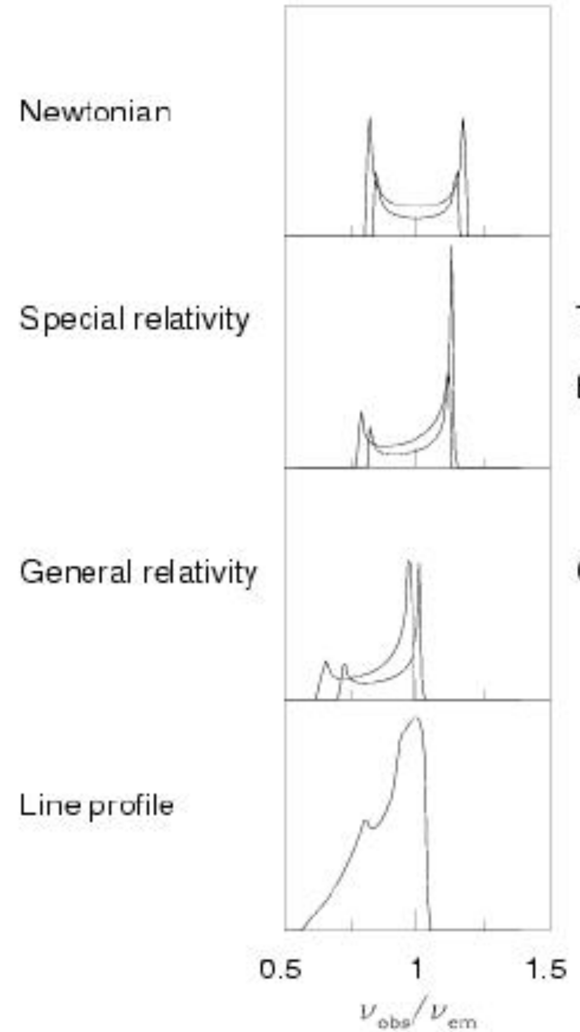

<u>REVIEWS</u> :

Fabian et al. 2000

Reynolds & Nowak 2003

Slide courtesy of Julia Lee

Diagnostic Tool: Black Hole Spin

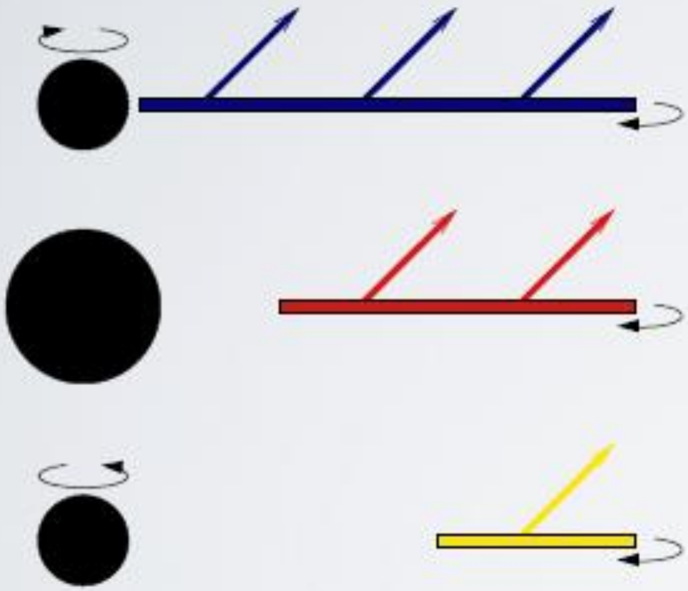

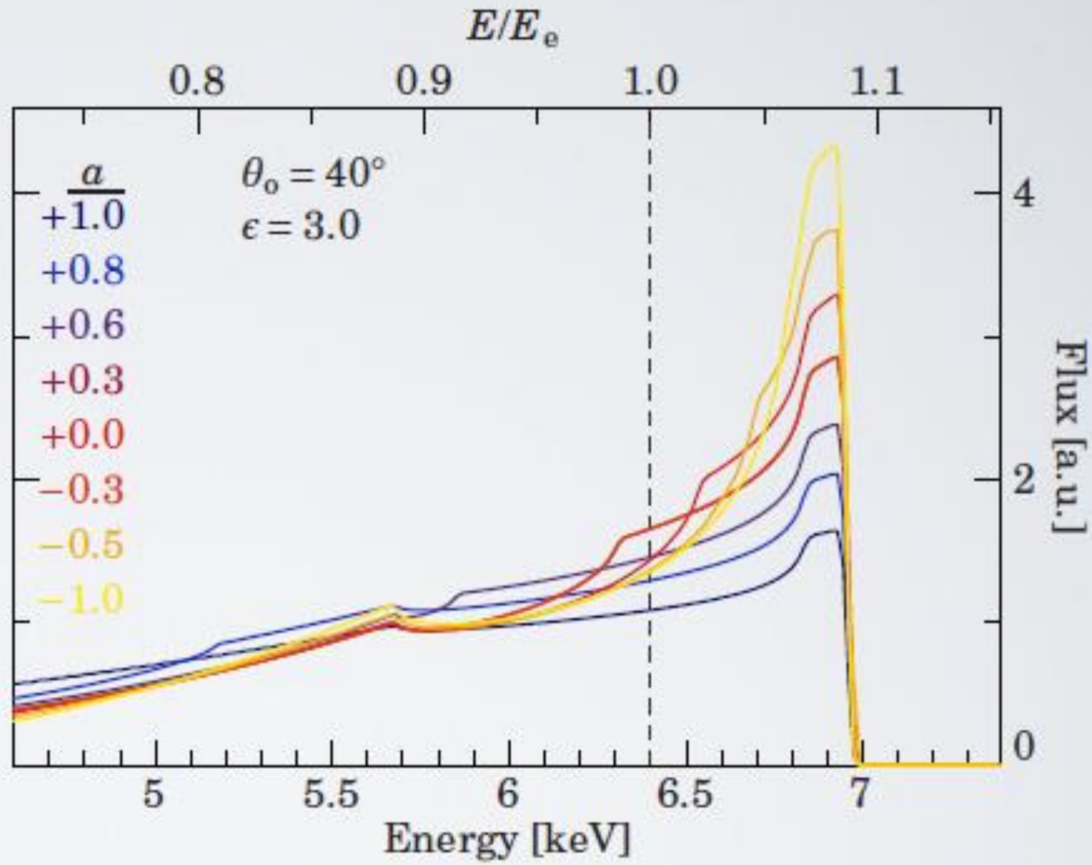

possible **Spin** values: $\mathbf{a} = -1 \ldots 1$

$a = cJ/GM^2$ (Dimensionless Spin Parameter)

The Problem of the Fe Abundance

Iron abundance determinations using reflection spectroscopy from publications since 2014 tend to find a few times the Solar value!

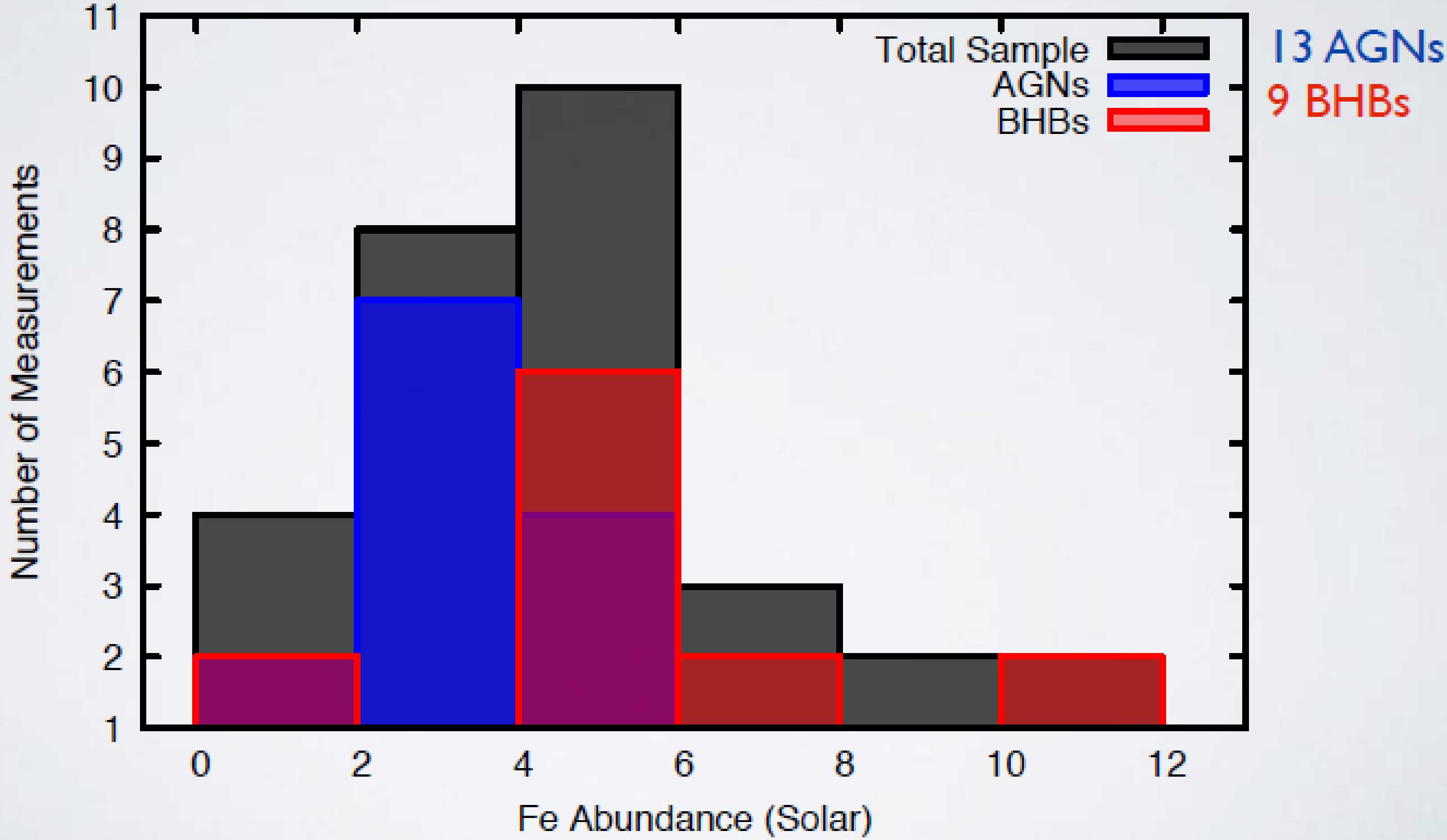

We have been including high-density effects (n_e > 15 cm-3) in XSTAR

- Continuum lowering (Debye-Hückel) – J Deprince PhD thesis
- DR suppression – based on expressions by Nikolić+13
- Three-body recombination – determined from collisional ionization cross sections (Raymond & Smith 77, Bryans+06) or hydrogenic rates otherwise
- Stimulated radiative processes – rates for recombination and decay enhanced by a factor $1 + \frac{F_e h^3 c^2}{2e^3}$
- Free-free heating – cut-off power law

Continuum lowering is treated with a Debye-Hückel potential
A universal formula was derived for the IP and K-edge shifts

$$H_{\mathrm{DC}}^{\mathrm{DH}} = \sum_i c\alpha_i \cdot \boldsymbol{p}_i + \beta_i c^2 - \frac{Z}{r_i} e^{-\mu r_i} + \sum_{i>j} \frac{1}{r_{ij}} e^{-\mu r_{ij}}, \qquad \mu = \frac{1}{\lambda_{\mathrm{D}}} = \sqrt{\frac{4\pi n_{\mathrm{e}}}{kT_{\mathrm{e}}}}.$$

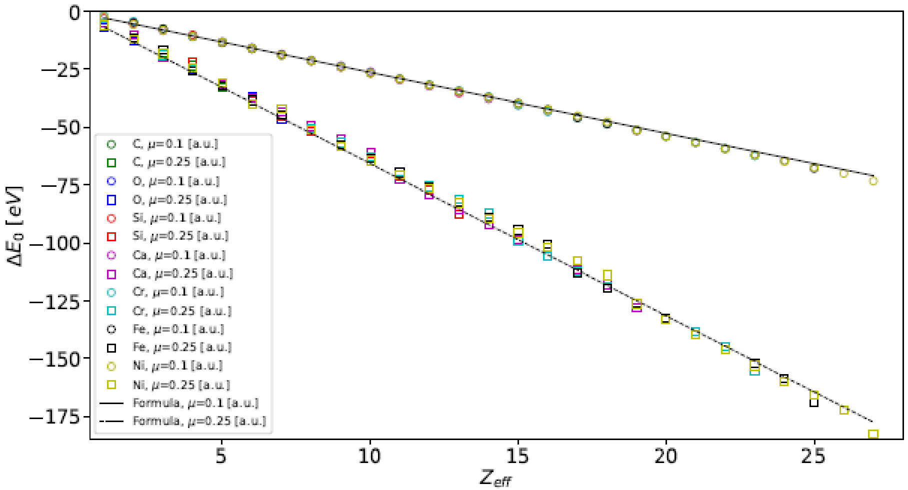

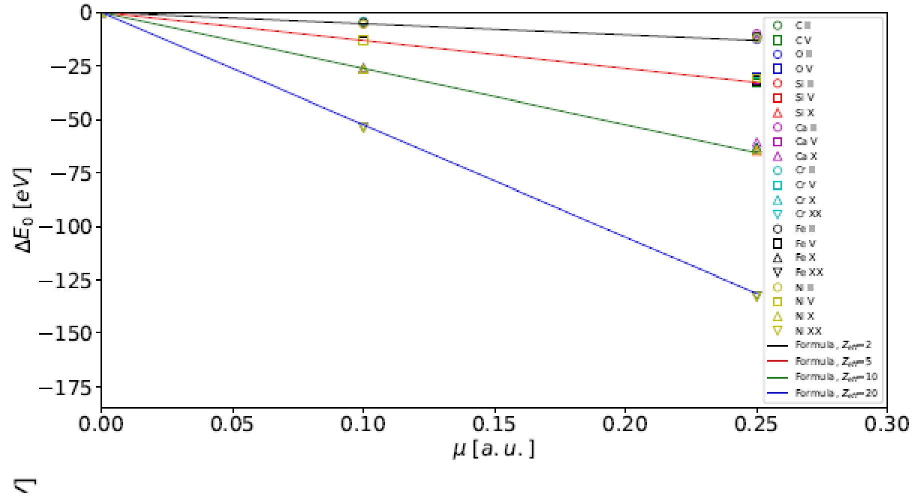

Figure from Palmeri+22

DB maintenance and poor user interaction have been chronic problems

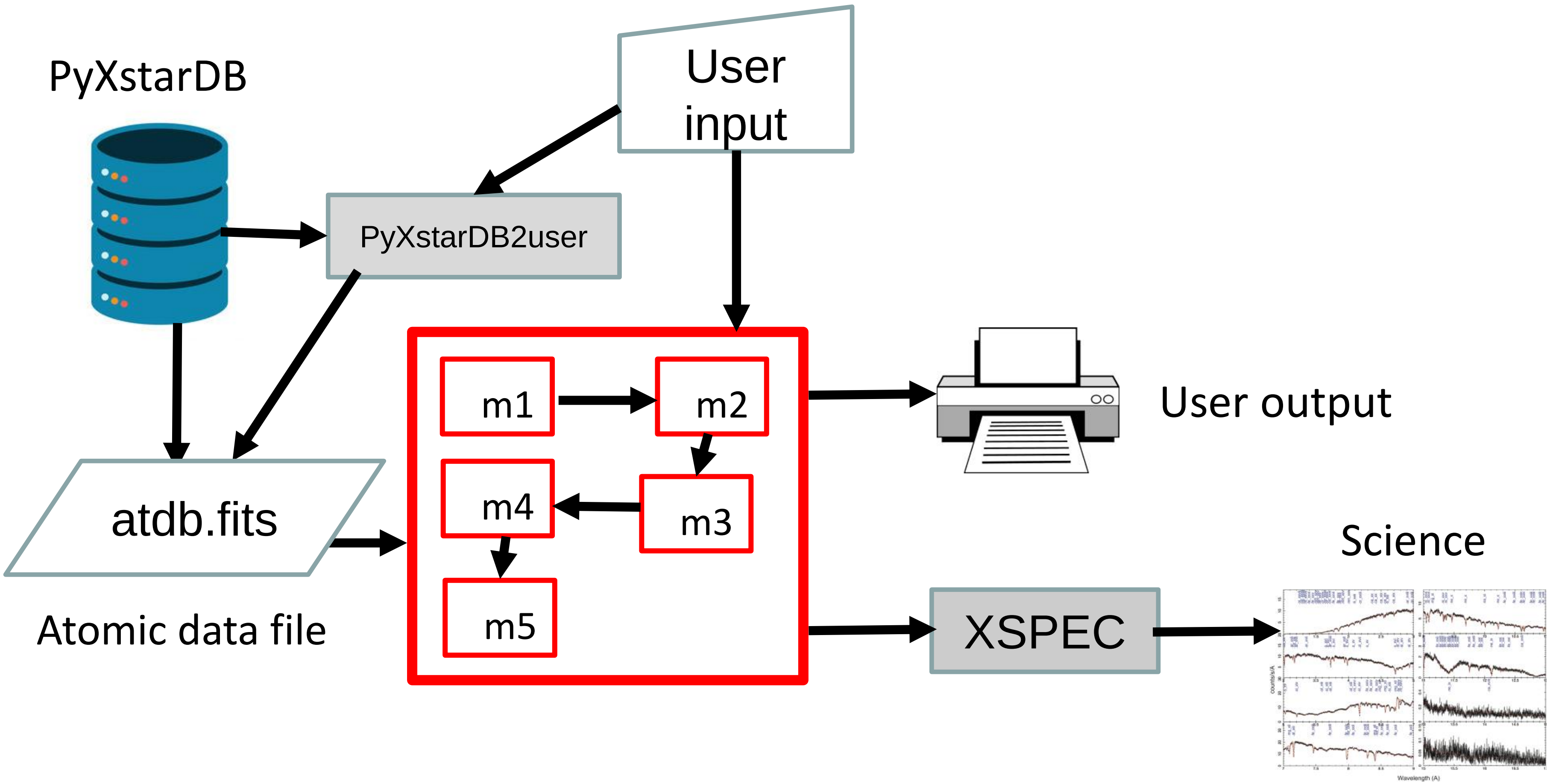

DB maintenance and poor user interaction have been chronic problems

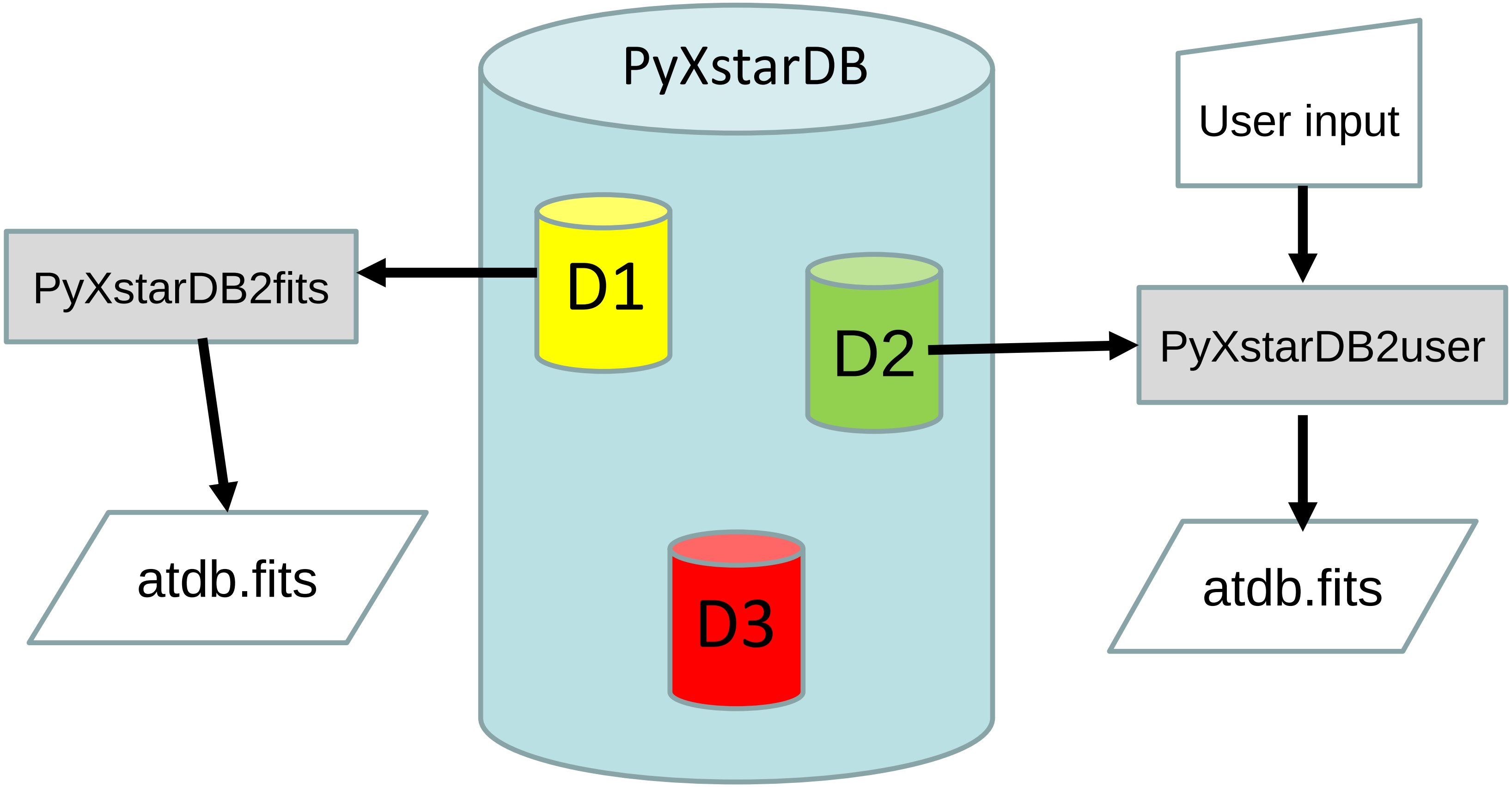

PyXstarDB and PyXstar are the new ventures

PyXstarDB (Kallman & Bautista):

- Open access to data producers and users (Jupyter notebooks)
- Effective and error-free database updates (SQLite)
- Automated updating from NIST and CHIANTI databases
- Ease of manipulation, queries, and intercomparisons (Pandas DF)
- Data preservation by avoiding the discard of outdated sets
- Sustainability

PyXstar (Kallman & Mendoza):

- XSTAR modernization under object-orientated programming (Fortran18)
- Wrap XSTAR Fortran modules as Python functions
- Allow user access to under-the-hood data (atomic and plasma data manipulation with Pandas DF & Astropy Tables)
- Comprehensive documentation and online user group